Cerebral Cortex, January 2019;29: 54–69

doi: 10.1093/cercor/bhx303
Advance Access Publication Date: 17 November 2017
Original Article

ORIGINAL ARTICLE

Astrocyte-Specific Deletion of *Sox2* Promotes Functional Recovery After Traumatic Brain Injury

Chunhai Chen[1,2,3,†], Xiaoling Zhong[1,2,†], Derek K. Smith[1,2], Wenjiao Tai[1,2], Jianjing Yang[1,2], Yuhua Zou[1,2], Lei-Lei Wang[1,2], Jiahong Sun[1,2], Song Qin[1,2,4,5] and Chun-Li Zhang[1,2]

[1]Department of Molecular Biology, University of Texas Southwestern Medical Center, 6000 Harry Hines Blvd, Dallas, TX 75390-9148, USA, [2]Hamon Center for Regenerative Science and Medicine, University of Texas Southwestern Medical Center, 6000 Harry Hines Blvd, Dallas, TX 75390-9148, USA, [3]Department of Occupational Health, Third Military Medical University, Chongqing 400038, China, [4]Department of Anatomy, Histology and Embryology, School of Basic Medical Sciences, Fudan University, Shanghai 200032, China and [5]Center of Neural Injury and Repair, Shanghai Tenth People's Hospital Affiliated with Tongji University, Shanghai 200072, China

Address correspondence to email: sqin@fudan.edu.cn (S.Q.) and Chun-Li.Zhang@UTSouthwestern.edu (C.-L.Z.).

[†]Denotes equal contribution.

Abstract

Injury to the adult brain induces activation of local astrocytes, which serves as a compensatory response that modulates tissue damage and recovery. However, the mechanism governing astrocyte activation during brain injury remains largely unknown. Here we provide in vivo evidence that SOX2, a transcription factor critical for stem cells and brain development, is also required for injury-induced activation of adult cortical astrocytes. Genome-wide chromatin immunoprecipitation-seq analysis of mouse cortical tissues reveals that SOX2 binds to regulatory regions of genes associated with signaling pathways that control glial cell activation, such as *Nr2e1*, *Mmd2*, *Wnt7a*, and *Akt2*. Astrocyte-specific deletion of *Sox2* in adult mice greatly diminishes glial response to controlled cortical impact injury and, most unexpectedly, dampens injury-induced cortical loss and benefits behavioral recovery of mice after injury. Together, these results uncover an essential role of SOX2 in somatic cells under pathological conditions and indicate that SOX2-dependent astrocyte activation could be targeted for functional recovery after traumatic brain injury.

Key words: brain repair, neural stem cell, reactive gliosis, SOX2, traumatic brain injury

Introduction

Traumatic brain injury (TBI) is primarily triggered by an external mechanical force. It induces a complex pathological process that includes glial activation, inflammation, cell death, and tissue loss (Xiong et al. 2013). At the cellular level, astrocytes are a principal cell type that contributes to glial response and inflammation, which ultimately regulates overall cell death and tissue damage (Sofroniew and Vinters 2010; Burda and Sofroniew 2014; Pekny and Pekna 2014). In response to injury, local astrocytes turn into an active form called "reactive astrocytes," characterized by changes in morphology and gene expression, cell cycle re-entry, and production of proinflammatory cytokines (Sofroniew 2009; Buffo et al. 2010). Astrocyte activation, or astrogliosis, plays a central role in the response to most

neurological diseases and traumatic injuries. These reactive astrocytes constitute a major cellular component of scar formation that is critical for wound healing and tissue remodeling in response to brain injury (Ridet et al. 1997; Bush et al. 1999). Thus, targeting specific genes that modulate reactive astrocytes will have important influences on the outcome of neural injury (Pardo et al. 2016).

SOX2 (Sex determining region of Y chromosome [Sry]-related high mobility group box 2) belongs to the SOX family of transcription factors (Gubbay et al. 1990). It is one of the earliest transcription factors expressed in neural stem cells, and plays a key role in specifying early neural lineages and brain development (Avilion et al. 2003; Bylund et al. 2003). In the adult, SOX2 is enriched in neurogenic regions of the brain, including the subventricular zone of the lateral ventricle and the subgranular zone of the dentate gyrus (Bylund et al. 2003; Graham et al. 2003; Ferri et al. 2004; Episkopou 2005). SOX2$^+$ cells are self-renewable and multipotent in the adult neurogenic niche (Suh et al. 2007). Outside of neural stem cell populations, SOX2 is detectable in proliferating astrocytes in the developing mouse brain and early postnatal astrocytes in culture (Bani-Yaghoub et al. 2006). Interestingly, its expression becomes silenced in astrocytes after long-term culture, but expression can be reactivated by injury or growth stimulation. This SOX2 reactivation accompanies astrocyte proliferation (Bani-Yaghoub et al. 2006). Nevertheless, not much is known about the expression and function of SOX2 in adult cortical astrocytes and its role under pathological conditions.

Here, we examined the expression and function of SOX2 in the adult brain under normal condition and after TBI. We found that SOX2 is constitutively expressed in postmitotic cortical astrocytes, and that its expression is greatly upregulated in response to TBI. Using an inducible knockout model of *Sox2* mutant mice, we also investigated its function in adult astrocytes. Although no obvious changes were detected in astrocyte survival and morphology or animal behaviors under normal conditions, injury-induced reactive astrogliosis was greatly dampened in *Sox2* mutant mice. Unexpectedly, *Sox2*-deletion significantly ameliorated injury-induced tissue loss and behavioral deficits, indicating that SOX2-mediated reactive astrogliosis is maladaptive to traumatic injury.

Materials and Methods

Animals

The following transgenic mice were used: *Sox2$^{f/f}$* (The Jackson Laboratory, stock 013093) (Shaham et al. 2009), *Aldh1l1-EGFP* (MMRRC, stock 011015-UCD) (Gong et al. 2003), *hGFAP-CreER^{T2}* (The Jackson Laboratory, stock 012849) (Ganat et al. 2006), *mGfap-Cre* (The Jackson Laboratory, stock 024098) (Gregorian et al. 2009), *Rosa-tdTomato* (Rosa-tdT; The Jackson Laboratory, stock 007914) (Madisen et al. 2010), and *Rosa-YFP* (The Jackson Laboratory, stock 006148) (Srinivas et al. 2001). Wild-type male C57BL/6J mice were purchased from The Jackson Laboratory. The *hGFAP-CreER^{T2}*, *Sox2$^{f/f}$*, and *Rosa-tdT* mice were bred together to generate *hGFAP-CreER^{T2}*; *Sox2$^{f/f}$*; *Rosa-tdT* mice. Mice were housed under a 12-h light/dark cycle with ad libitum access to food and water in a controlled animal facility. Adult male and female mice at 6 weeks of age and older were used unless otherwise stated. No overt gender-associated mutant phenotype was observed. Experimental procedures and protocols were approved by the Institutional Animal Care and Use Committee at UT Southwestern Medical Center.

Tamoxifen and BrdU Treatments

Tamoxifen (T5648; Sigma) was dissolved in a mixture of ethanol and sesame oil (1:9 by volume) at a concentration of 40 mg/ml. Tamoxifen was given by intraperitoneally injection at a daily dose of 1 mg/10 g body weight for 3–5 days. Mice were analyzed at least 7 days post tamoxifen treatments. BrdU (B5002; Sigma; 1 g/l) was supplied in drinking water for durations as indicated in the text.

Controlled Cortical Impact Injury

The controlled cortical impact (CCI) model of TBI was employed. Under anesthesia, a skin incision was made in the mouse forehead to expose the skull. A craniotomy was performed over the right hemisphere and the bone flap (2.2 mm in diameter) was carefully removed. A cortical injury (0 bregma, 1 mm lateral to the sagittal suture line) was introduced at an impact depth of 1 mm with a 2-mm diameter round impact tip (speed 3.0 m/s, dwell time 100 ms) by using an electromagnetically driven CCI device (Impact One^{TM} Stereotaxic CCI Instrument, Leica). Both motor and sensory cortices were impacted. After injury, the skin was sutured and further secured with liquid adhesive.

Behavior Tests

In accordance with previous publications on TBI (Schwarzbold et al. 2010; Washington et al. 2012; Tweedie et al. 2013; Kondo et al. 2015), we chose a battery of behavior paradigms to examine neurological functions associated with the injured cortical area. All animals were encoded before tests. Their behaviors were evaluated by 2 observers who were blinded to the experimental conditions and treatments. Data were collected and then decoded for group analyses. Nine or more mice were included in each experimental group.

Modified neurologic severity scores (mNSS): mNSS was used to exam the overall neurologic functions of mice before and 1, 7, 14, 21, and 28 days after injury. mNSS was graded on a scale of 0–14 as previously described with modifications (normal score 0; maximal deficit score 14, for details see Supplementary Table S4) (Chen et al. 2005). The mNSS value correlates with impairment severity.

Elevated plus maze: An elevated plus maze was used to assess risk-taking behavior of mice 5 weeks after injury as previously described (Walf and Frye 2007; Kondo et al. 2015). Briefly, the maze consisted of 4 arms in a "plus" shape formation. The 2 open arms have no wall and the 2 closed arms have surrounding walls (30 × 5 × 15 cm^3) and an open top. The entire maze is raised 85 cm above the floor. Mice are placed in the center of the maze, facing one of the open arms, and allowed to explore the maze for a total of 5 min. The total time spent in the 2 closed and the 2 open arms was recorded and used as a surrogate measure of risk-taking behavior; mice that spent less time in the open arms were considered to have lower levels of risk-taking behavior.

Tail suspension test: The tail suspension test was used to measure behavioral despair. We carried out tail suspension test 6 weeks after injury using a methodology described previously (Can et al. 2012). Briefly, the mice were suspended by the tail using adhesive tape 50 cm above the floor for 6 min. The immobility time of each mouse—with immobility defined as hanging passively, without active movements—was recorded. An increased immobility time is considered as depression-like behavior.

Morris water maze: Morris water maze (MWM) was used to evaluate spatial learning and memory under normal condition or 8 weeks after injury as previously described (Zhang et al.

2008). Mice were trained 4 trials per day for 10 days. The probe trial was conducted 24 h after the last learning session. The entire procedure in the pool was monitored by an automatic tracking system to record swim speed, time to platform, total distance moved, and time spent in the target quadrant where the platform was previously located.

Immunohistochemistry

Mice were euthanized with CO_2 overdose and intracardially perfused with ice-cold PBS and 4% paraformaldehyde (PFA) in PBS. Brains were collected and postfixed with 4% PFA overnight at 4 °C. Then the brain samples were cryoprotected with 30% sucrose solution in PBS for 24 h and cut into 40-μm-thick sections. Sections were serially collected and stored in anti-freezing solution at −20 °C. Immunohistochemistry was performed as previously described (Niu et al. 2013). The following primary antibodies were used: GFAP (G3893; mouse; 1:500; Sigma), BrdU (OBT0030; rat BU1/75; 1:500; Accurate Chemical), SOX1 (4194 S; rabbit; 1:500; Cell Signaling Technology), SOX2 (Sc-17320; goat; 1:200; Santa Cruz), SOX3 (rabbit; 1:200; a gift from M. Klymkowsky (Wang et al. 2006)), RBFOX3 (MAB377, mouse, 1:500, Millipore), OLIG2 (AB9610; rabbit; 1:500; Millipore), NG2 (MAB5384; mouse; 1:500; Millipore), IBA1 (019-19741; rabbit; 1:500; Waco), ALDC (sc-12065; goat; 1:200; Santa Cruz), ALDH1L1(75-140; mouse; 1:50; NeuroMab), GS (MAB302; mouse; 1:50; Chemicon), KI67 (LS-C121244; rabbit; 1:200; Lifespan Biosciences), and GFP (detecting both GFP and YFP, chick, 1:500, Aves Labs). Alexa Fluor 488-, 555-, or 647-conjugated corresponding secondary antibodies from Jackson ImmunoResearch were used for indirect fluorescence. Cell nuclei were counterstained with Hoechst33342 (Ho) when appropriate. Images were taken using a Zeiss LSM700 confocal microscope. A Cell Counter software plugin in the ImageJ program was used to count cells. Data were obtained from 12 random sections from 3 to 6 mice in each group.

Quantification of Reactive Gliosis and Lesion Size After Injury

Reactive gliosis was examined as described previously (Clausen et al. 2011; Kang et al. 2014). Briefly, one-third of the brain sections spanning the whole injury cortex of each mouse were used for quantification. Reactive gliosis indicated by $GFAP^+$ area was measured by using the Stereo Investigator software (MBF Bioscience) under identical imaging parameters with a fluorescent microscope. In each slice, the $GFAP^+$ area was quantified from above the top edge of the corpus callosum to the edge of lesion area with the same threshold of fluorescent intensity. The total $GFAP^+$ area for each mouse was then calculated as the following: total $GFAP^+$ area = $(\sum_{i=1}^{n} GFAP^+ \text{ area}) \times 3$. Brain lesion size was determined as previously described (Myer et al. 2006). Briefly, one-sixth of the brain sections spanning the whole injury cortex of each mouse were used for quantification. Borders between healthy and degenerated cortex were generally sharp and clearly defined by Hoechst33342 staining. Areas of healthy cortical tissues on the ipsilateral and contralateral sides were measured with ImageJ and were used to calculate relative lesion size as a ratio of the 2 sides.

Chromatin Immunoprecipitation and Sequencing

The cortices of wild-type mice were dissected on ice and cut into small pieces. After isolation, these cortical tissues were incubated for 20 min at RT with 10 ml of long-arm cross-linker solution consisting of 15 mM Hepes-Cl (pH 7.6), 60 mM KCl, 15 mM NaCl, 0.34 M sucrose, 2 mM $MgCl_2$, and freshly added 1.5 mM ethylene glycol bis (succinimidyl succinate, EGTA) and 1 tab/10 mL EDTA-free protease inhibitor tablet. The tissues were crosslinked with 5 volumes of freshly prepared solution (1% formaldehyde, 50 mM Hepes-KOH (pH 7.5), 100 mM NaCl, 1 mM EDTA, and 0.5 mM EGTA) for 12 min at RT. The reaction was quenched with 1/20 volume of 2.5 M glycine followed by 2 washes with ice-cold PBS. Subsequently, the tissues were dounced in ice-cold PBS first with a loose and later with a tight pestle, followed by filtration through a 100-μm cell strainer to remove connective tissues. Dissociated cells were collected by centrifugation at 2000 rcf for 5 min at 4 °C. Cell pellets were resuspended in 10 ml of lysis buffer I (50 mM HEPES-KOH [pH 7.5], 140 mM NaCl, 1 mM EDTA, 10% Glycerol, 0.5% Igepal CA-630, 0.25% Triton X-100, and protease inhibitor). After incubation with gentle rocking for 10 min at 4 °C, cells were collected by centrifugation at 2000 rcf for 4 min at 4 °C. Pellets were resuspended in 10 ml of lysis buffer II (10 mM Tris–HCL [pH 8.0], 200 mM NaCl, 1 mM EDTA, 0.5 mM EGTA, and protease inhibitor) and incubated with gentle rocking for 5 min at 4 °C. Nuclei were collected by spinning at 2000 rcf for 5 min at 4 °C and resuspended in shearing buffer (50 mM HEPES [pH 8.0], 10 mM EDTA [pH 8.0], 1% SDS, EDTA-free complete protease inhibitor). Chromatin was sheared for 45 min with 30 s ON and 30 s OFF cycles until DNA fragments were 200–600 bp. Immunoprecipitation was performed using anti-SOX2 (AB5603, rabbit, 5 μg, Millipore) as previously described (Islam et al. 2015). Chromatin immunoprecipitation (ChIP) experiments were repeated in triplicate and 3 mice were used for each immunoprecipitation reaction. ChIP-seq libraries were generated using a NEBNext ChIP-Seq Library Prep Master Mix Set for Illumina (New England Biolabs, E6240S) with NEBNext Multiplex Oligos for Illumina (New England Biolabs, E7335S). Briefly, 5 ng purified chromatin and 5 ng purified immunoprecipitated chromatin were used for ChIP-seq library construction. Replicate libraries were prepared from 3 independent immunoprecipitations. Single-end 50-base length sequencing reads were generated on an Illumina HiSeq 2500 System. Reads were aligned to the mouse reference sequence GRCm38/mm10 with the Bowtie algorithm. Peak calling, peak-gene annotation, and motif discovery (parameter: 200 nucleotide window from peak center) were performed using HOMER (version 4.7). Gene ontology classification was performed using HOMER and Wikipathway analysis (version 2.0.2). The UCSC Genome Browser was used to visualize tag densities and multiexperiment datasets. The dataset GSE85213 was submitted to the Gene Expression Omnibus (GEO) data repository.

Primary Astrocyte Culture and 4-OH-Tamoxifen Treatment

We isolated primary cortical astrocytes from individual postnatal day 1 (P1) to P2 pups of *hGFAP-CreER*^{T2}; *Sox2*$^{f/f}$; *Rosa-tdT* mice as previously described (Schildge et al. 2013). After genotyping, we combined cells with the same genotype and cultured them in DMEM high glucose with 10% of FBS. We removed loosely attached microglia/macrophages and oligodendrocyte precursor cells from the cell monolayer by vigorous shaking or blasting with medium through a 10 ml pipette. Cells were passaged and cultured in vitro for 3 weeks with medium change every 3 days. We then treated the cells for 3 days with daily change of fresh medium containing 1 μM 4-OH-tamoxifen. Cells were then collected for analysis.

Isolation of Adult Cortical Astrocytes

We used a sucrose density centrifugation and immunopanning to purify adult astrocytes from cortical tissues at 3 days post CCI injury. Briefly, we dissected the cortical tissues surrounding the injury area in ice-cold PBS and transferred them into 1.5 ml Eppendorf tubes containing 1 ml warm PPD solution (200 µl Papain, 10.4 mg DNase I, 200 mg Dispase II in 100 ml DMEM high glucose medium). We dissociated the tissues through pipetting with a 1 ml tip for 10 times, incubated for 15–20 min with occasional mixing at 37 °C, and dissociated again through pipetting. We then collected cells through centrifugation for 3 min at 500 rcf and resuspended them into 10 ml PBS with 30% sucrose and 3% FBS. This cell mixture was filtered through a 40-µm mesh into a 50-ml tube. After a 30-s spin at 1000 rcf, the supernatant was transferred to a new tube and further centrifuged for 1.5 min at 1000 rcf to collect cell pellets. Cells were then resuspended in 4 ml PBS containing 0.02% BSA/DNase and subjected to immunopanning. Panning petri dishes were prepared ahead of cell isolation. Each 6-cm petri dish was coated with 4 ml secondary antibody-containing 50 mM Tris–HCl (pH 9.5) buffer. The "secondary antibody-only" dish was coated with buffer containing 12 µg of donkey anti-goat IgG (H + L) antibody, while the "CD45" dish was coated with buffer containing 12 µg of goat anti-rat IgG (H + L) antibody (Jackson ImmunoResearch). After overnight incubation at 4 °C, these dishes were then washed 3 times with PBS. The "secondary antibody only" dish was further coated with 2.4 ml PBS with 0.2% BSA/DNase, while the "CD45" dish was coated with the above buffer containing 0.2 µg of rat anti-mouse CD45 (BD Biosciences). These dishes were incubated for at least 2 h at RT before use. For immunopanning, cells were first added to "secondary antibody only" dishes, which were gently swirled to evenly distribute the cells. After sitting for 10 min, the dishes were gently shaken and then incubated for another 10 min. The unbound cells (the supernatant) were transferred to the "CD45" dishes for further panning with the same method. The final unbound cells—predominantly astrocytes—were transferred to a 10 ml conical tube and collected by spinning for 3 min at 200 rcf at RT. Cell pellets were then directly lysed in 1 ml Trizol regent for RNA isolation.

Quantitative RT-PCR

Total RNAs were extracted from cells with Trizol regent. qRT-PCR was performed with SYBR Green chemistry and primers listed in Supplementary Table S3.

Statistical Analysis

Experiments were routinely repeated at least 3 times and the repeat number was increased according to sample variations. Data were analyzed using GraphPad Prism 6 software and presented as means ± standard error of the mean (S.E.M.). Pairwise comparisons were analyzed by two-tailed Student's *t*-test. One-way ANOVA with Tukey's post hoc test was used for 3 or more independent variables. Two-way ANOVA and post hoc Tukey's test were used for mNSS and Morris water maze. A P value < 0.05 was considered significant.

Results

Astrocyte-Enriched Expression of SOX2 in the Adult Cortex

SOX2 plays critical roles during neural development (Bylund et al. 2003; Tanaka et al. 2004); however, its function in adult non-neurogenic brain regions is not clear. We first examined SOX2 expression through immunohistochemistry. Both western blotting and immunocytochemistry confirmed that the antibody specifically recognizes SOX2 but not the closely related SOX1 or SOX3 (Supplementary Fig. S1a, b). Interestingly, SOX2 was broadly detectable in the adult mouse cortex (Supplementary Fig. S1c), although only 7% is RBFOX3$^+$ neurons and the expression in these cells is generally much weaker (Fig. 1*a*, arrowhead). SOX2 expression in astrocytes were determined in *Aldh1l1-EGFP* mice, in which GFP expression is controlled by regulatory elements for the astrocyte-enriched *Aldh1l1* gene (Tsai et al. 2012). Quantification showed that approximately 63.8% of SOX2$^+$ cells express GFP (Fig. 1*b*).

SOX2 expression in astrocytes was further confirmed with the specific marker glutamine synthetase (GS; Fig. 1*b*). Over 60% of SOX2$^+$ cells express GS, whereas only 16% of the population express OLIG2, a marker for oligodendrocytes and oligodendrocyte precursor cells (Fig. 1*b*, *c*). SOX2 expression, nonetheless, is relatively lower in OLIG2$^+$GFP$^-$ cells than in neighboring OLIG2$^-$GFP$^+$ cells (Fig. 1*c*, arrows and arrowheads; the ratio of SOX2 fluorescence intensity in OLIG2$^-$GFP$^+$ vs. OLIG2$^+$GFP$^-$ = 3.3, $n = 50$, $P < 0.0001$). In sharp contrast, SOX2 was not observed in IBA1$^+$ cells, a microglia/macrophage-restricted marker (Fig. 1*d*). To determine whether aging influences SOX2 expression patterns, we compared SOX2 expression in both young (2 months old) and aged (24 months old) mice. No significant difference was identified in either the cellular distributions or expression levels (Fig. 1*b*, *c*, *e*). Together, these data reveal that SOX2 is predominantly expressed in cortical astrocytes and its expression is not much altered during the aging process.

Identification of Genome-Wide SOX2-Binding Sites in the Adult Cortex

The role of SOX2 is well established in neural stem cell regulation and development of the nervous system (Suh et al. 2007; Pevny and Nicolis 2010); however, not much is known about how SOX2 functions in the adult cortex. We performed ChIP-seq using adult mouse cortical tissue to define the genome-wide binding patterns of SOX2. Bioinformatic analysis revealed 9334 bound sites that are shared between three biologically independent samples. Among these, 2114 high-fidelity sites have a peak score ≥ 10. A de novo motif search identified motifs enriched within each dataset. The 2 most enriched motifs resemble the canonical SOX binding site or HMG-box (Fig. 2*a*). Two variants of this HMG-box together represented more than 80% of the searched target sequences. The second most enriched motif is annotated to POU factors, which were previously shown as cofactors of SOX family transcription factors (Tanaka et al. 2004). Approximately 43% of searched target sequences contain this POU-binding motif (Fig. 2*a*). These results strongly validate the high quality of our SOX2 ChIP-seq datasets and suggest that many genes may be co-regulated by SOX2 and POU factors.

SOX2-bound sites are mainly localized to intronic (41.3%), intergenic (36.1%), and promoter-transcription start site (19.2%) regions (Fig. 2*b*). Among the genes annotated to SOX2-bound elements, numerous have been implicated in astrogliosis and reactive astrocyte proliferation after TBI or other brain diseases, such as *Nr2e1*, *Mmd2*, *Wnt7a*, *and Akt2* (Fig. 2*c*, and Supplementary Table S1). Interestingly, the SOX2-binding site in the *Nr2e1* locus was previously identified to be functional in a transgenic enhancer analysis (Islam et al. 2015), further confirming the specificity and fidelity of our ChIP-seq results. To globally assess the function of SOX2 targeted genes, we

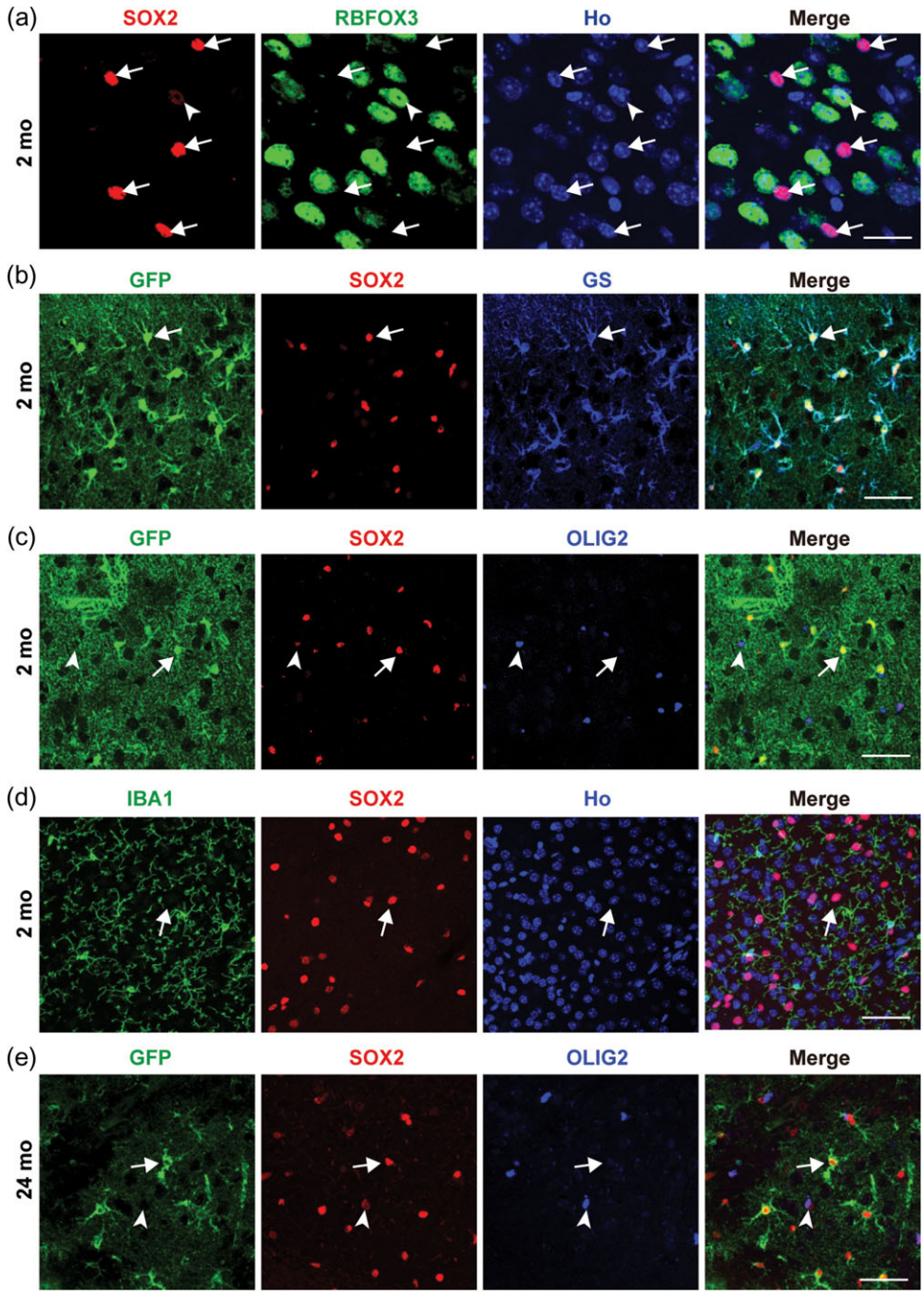

Figure 1. SOX2 expression in adult mouse cortex. (*a*) Rare and weak SOX2 expression in cortical neurons (indicated by an arrowhead). Non-neuronal expression is generally much stronger (indicated by arrows). (*b*) SOX2 expression in cortical astrocytes of *Aldh1l1-EGFP* mice. Astrocytes were identified by GS and the reporter GFP. Arrows show a representative $GFP^+GS^+SOX2^+$ cell. mo, month. (*c*) SOX2 expression in cortical $OLIG2^+$ oligodendrocytes or oligodendrocyte precursors of *Aldh1l1-EGFP* mice. Arrows show a representative $SOX2^{high}OLIG2^-GFP^+$ cell, whereas arrowheads show a representative $SOX2^{low}OLIG2^+GFP^-$ cell. SOX2 expression is always weaker in $OLIG2^+$ cells. (*d*) SOX2 is not expressed in $IBA1^+$ microglia. A representative $SOX2^+IBA1^-$ cell is indicated by an arrow. (*e*) SOX2 expression in cortical GFP^+ astrocytes (indicated by an arrow, $SOX2^{high}OLIG2^-GFP^+$) or $OLIG2^+$ cells (indicated by an arrowhead, $SOX2^{low}OLIG2^+GFP^-$) of 24-month-old *Aldh1l1-EGFP* mice. Scale bars: 25 μm (*a*) and 50 μm (*b*–*e*).

performed gene ontology (GO) analysis of all the genes with a peak score ≥10 using HOMER and Wikipathway analysis. An extensive list of enriched GO terms is presented in Supplementary Table S2. Importantly, the most enriched GO terms related to astrogliosis including the WNT signaling pathway (WP539), the Delta-Notch signaling pathway (WP265), the TGF-β signaling pathway (WP113), the IL-6 signaling pathway (WP387), and the MAPK signaling pathway (WP493) (Fig. 2*d*, and Supplementary Table S2). We confirmed through quantitative RT-PCR (qRT-PCR) analysis that expression of genes involved in astrogliosis was largely altered upon *Sox2* deletion in cultured astrocytes (Supplementary Fig. S2, Supplementary Table S3). These results suggest that SOX2 regulates astrocyte function by directly targeting components of multiple signaling pathways.

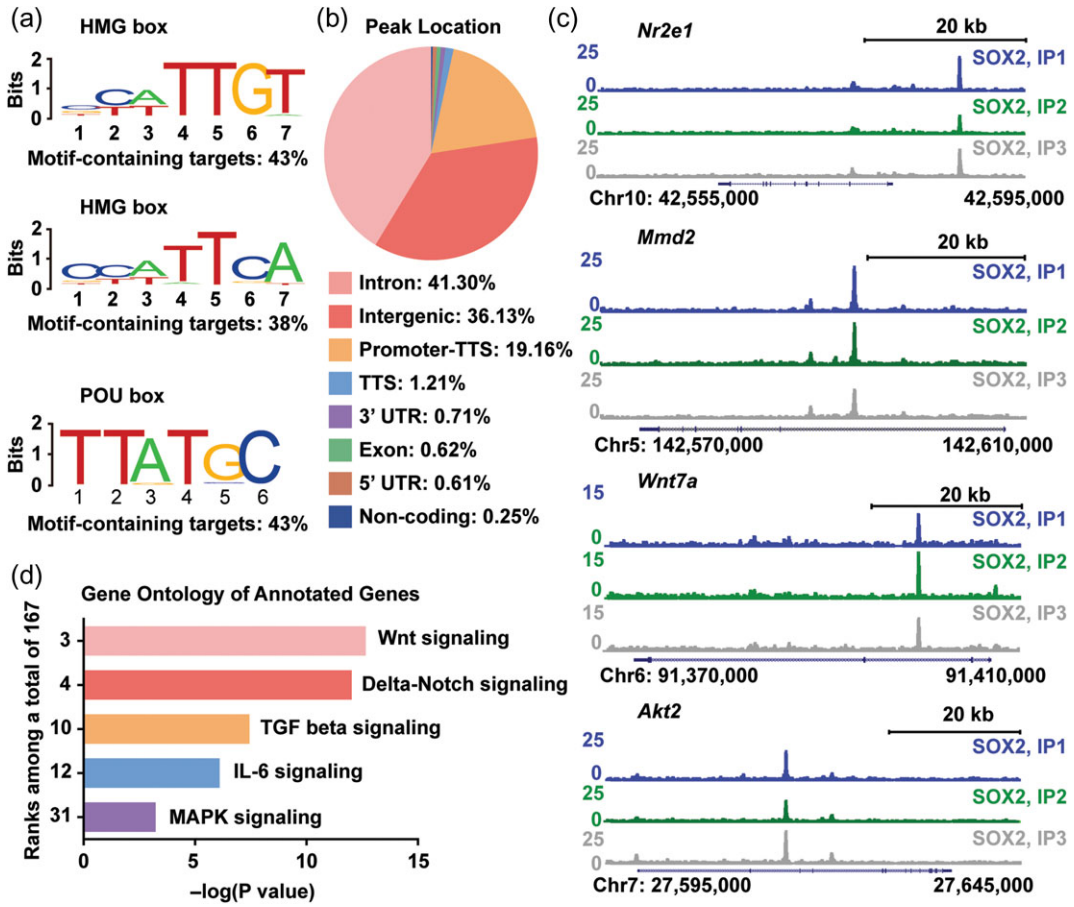

Figure 2. ChIP-seq analysis to reveal SOX2-regulated genes in the adult mouse cortex. (*a*) The predominant SOX2-bound motifs identified by genome-wide ChIP-seq analysis. (*b*) Genome-wide distribution of SOX2-binding peaks. (*c*) Representative genes directly targeted by SOX2. ChIP-seq was performed in triplicates using independent cortical tissues. (*d*) Highly enriched Gene Ontology terms by Wikipathway analysis.

Minimal Effect of *Sox2*-Deletion on Astrocytes and Animal Behaviors Under Homeostasis

To examine SOX2 function in adult astrocytes in vivo, we generated *hGFAP-CreER*^{T2}; *Sox2*$^{f/f}$; *Rosa-tdT* mice, in which the floxed alleles of *Sox2* can be conditionally deleted in astrocytes that are simultaneously marked by the Cre-dependent reporter tdTomato (tdT) (Fig. 3a). For simplicity, this *Sox2* mutant line is hereafter referred as *Sox2*-cKO. The floxed allele-negative mice were used as wild-type controls and dubbed *Sox2*-WT. The adult mice were intraperitoneally injected with tamoxifen for 4 days and analyzed 7 days after the final injection. Immunohistochemistry confirmed an efficient deletion of SOX2 expression in cortical astrocytes of adult *Sox2*-cKO mice (Fig. 3*b*,*c*). Unexpectedly, the adult *Sox2*-cKO brains did not show any gross morphological abnormalities when compared with *Sox2*-WT littermate controls even at 3 months following tamoxifen injections. Quantification of cortical astrocytes failed to reveal any obvious changes in cell density in *Sox2*-cKO mice (Fig. 3*d*, *e*). Astrocyte morphology also remained similar between wild-type controls and *Sox2*-cKO mice (Fig. 3*d*, *f*, *g*). Nonetheless, due to its expression in adult neural stem cells, *Sox2* mutant mice showed a mild but significant reduction of neurogenesis in the dentate gyrus and lateral ventricle (Supplementary Fig. S3).

We then examined whether *Sox2*-deletion led to any changes on animal behavior through a series of tests (Supplementary Fig. S4a). The overall neurological function was assessed through a modified neurological severity score (mNSS) system, which mainly measures reflex and body coordination (Supplementary Table S4). Both *Sox2*-cKO mice and wild-type controls performed equally well as indicated by an average score of 1–1.5 during a time course analysis (Fig. 3*h*). A two-way ANOVA and post hoc multiple comparisons failed to reveal any significant difference between experimental groups. The depression-like behavior was examined by tail suspension test (Fig. 3*i*). The average duration in immobility was around 120 s during a 6-min test session; and no significant difference was identified between wild-type and *Sox2*-cKO mice. Risk-taking and anxiety-like behavior was monitored by elevated plus maze. Similarly, we failed to observe any significant deficits in mice with *Sox2-cKO* (Fig. 3*j*). In addition, spatial learning and memory examined by the Morris water maze was also similar between wild-type and *Sox2*-cKO mice (Supplementary Fig. S4b, c). Together, these data indicate that SOX2 is not required for astrocyte survival and morphology. It also has no significant influence on cognitive and emotional behaviors of mice under normal condition.

Robust Response of SOX2$^+$ Cells to TBI

We used a CCI-induced TBI model to examine a potential role of SOX2 under pathological conditions (Fig. 4a). A time course analysis showed that CCI induced a rapid increase of both the number of SOX2$^+$ cells and the intensity of SOX2 expression

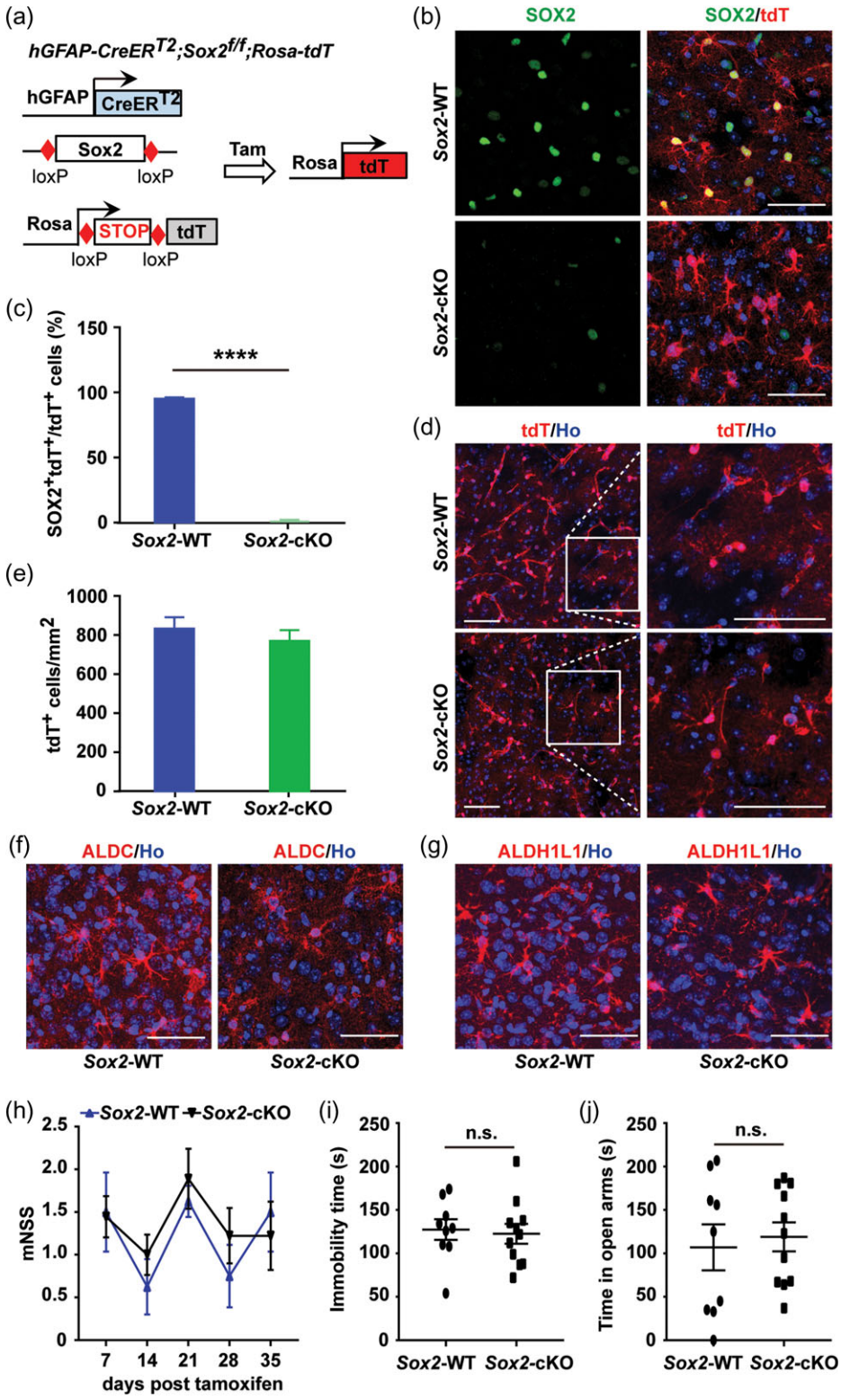

Figure 3. Lack of overt effects of SOX2-deletion on adult quiescent astrocytes. (*a*) An inducible approach to specifically delete *Sox2* in adult astrocytes. tdT, tdTomato. Tam, tamoxifen. (*b*) Representative confocal images showing deletion of SOX2 in tdT-traced astrocytes. (*c*) Quantification showing robust deletion of SOX2 in cortical astrocytes (means ± S.E.M., $n = 3$ mice, $^{****}P < 0.0001$ by *t*-test). (*d*) Morphology and density of cortical astrocytes traced by tdT with or without *Sox2*-deletion. Enlarged views of the boxed regions are also shown. (*e*) Quantification of astrocyte density in the adult cortex (means ± S.E.M.; $n = 3$ mice). (*f*, *g*) Morphology of cortical astrocytes examined by staining of the astrocyte-specific markers ALDC and ALDH1L1. (*h*) Overall neurological function determined by mNSS (means ± S.E.M.; $n = 9$ and 11 for WT and cKO mice, respectively; no significant difference between groups by two-way ANOVA analysis). (*i*) Tail suspension test to examine depression-like behavior (means ± S.E.M.; $n = 9$ and 11 for WT and cKO mice, respectively; n.s., not significant by *t*-test). (*j*) Elevated plus maze test to examine risk-taking and anxiety-like behavior (means ± S.E.M.; $n = 9$ and 11 for WT and cKO mice, respectively; n.s., not significant by *t*-test). Scale bars: 50 μm.

surrounding the injury site (Fig. 4*b–d*). Such increase was then much reduced at 28 days post CCI. Most importantly, we found that over 20% of those SOX2$^+$ cells surrounding the injury area expressed the cell proliferation marker KI67, indicating that a significant fraction of these cells entered cell cycle after injury (Fig. 4*e*, *f*).

CCI leads to reactive gliosis, including activation of astrocytes, microglia, and NG2$^+$ glia (Susarla et al. 2014). We analyzed each of these cell types for SOX2 expression 3 days post-CCI. To facilitate detection, cortical astrocytes were traced in *mGfap-Cre*; *Rosa-YFP* mice (Srinivas et al. 2001; Gregorian et al. 2009). These cortical YFP$^+$ cells strongly expressed SOX2 and nearly all expressed the reactive astrocyte marker GFAP (Fig. 5*a*). The ratio of SOX2$^+$YFP$^+$ cells among all cortical SOX2$^+$ cells increased from 60% in the noninjured condition to over 80% after CCI (Fig. 5*b*). This significant increase confirmed a specific response of SOX2$^+$ astrocytes to CCI.

Although CCI induced robust activation of microglia/macrophages as indicated by morphological change and upregulated IBA1 expression, no microglia/macrophage stained positive for SOX2 (Fig. 5*c*). CCI also did not cause misexpression of SOX2 in RBFOX3$^+$ neurons (Supplementary Fig. S5). Nonetheless, NG2$^+$ or OLIG2$^+$ cells were detected surrounding the injury site, many of which expressed SOX2 (Fig. 5*d*, *e*; arrows). These cells represented 20–30% of total SOX2$^+$ cells in the injured cortex (Fig. 5*f*, *g*). Interestingly, nearly all SOX2$^+$NG2$^+$ cells were also YFP$^+$ and more than 60% of SOX2$^+$OLIG2$^+$ cells were labeled by YFP (Fig. 5*d*, *e*), indicating that a fraction of astrocytes expressed NG2 and/or OLIG2 after CCI. Nonetheless, SOX2$^+$GFP$^+$ cells were the predominant cells surrounding the injury site with an overall density of

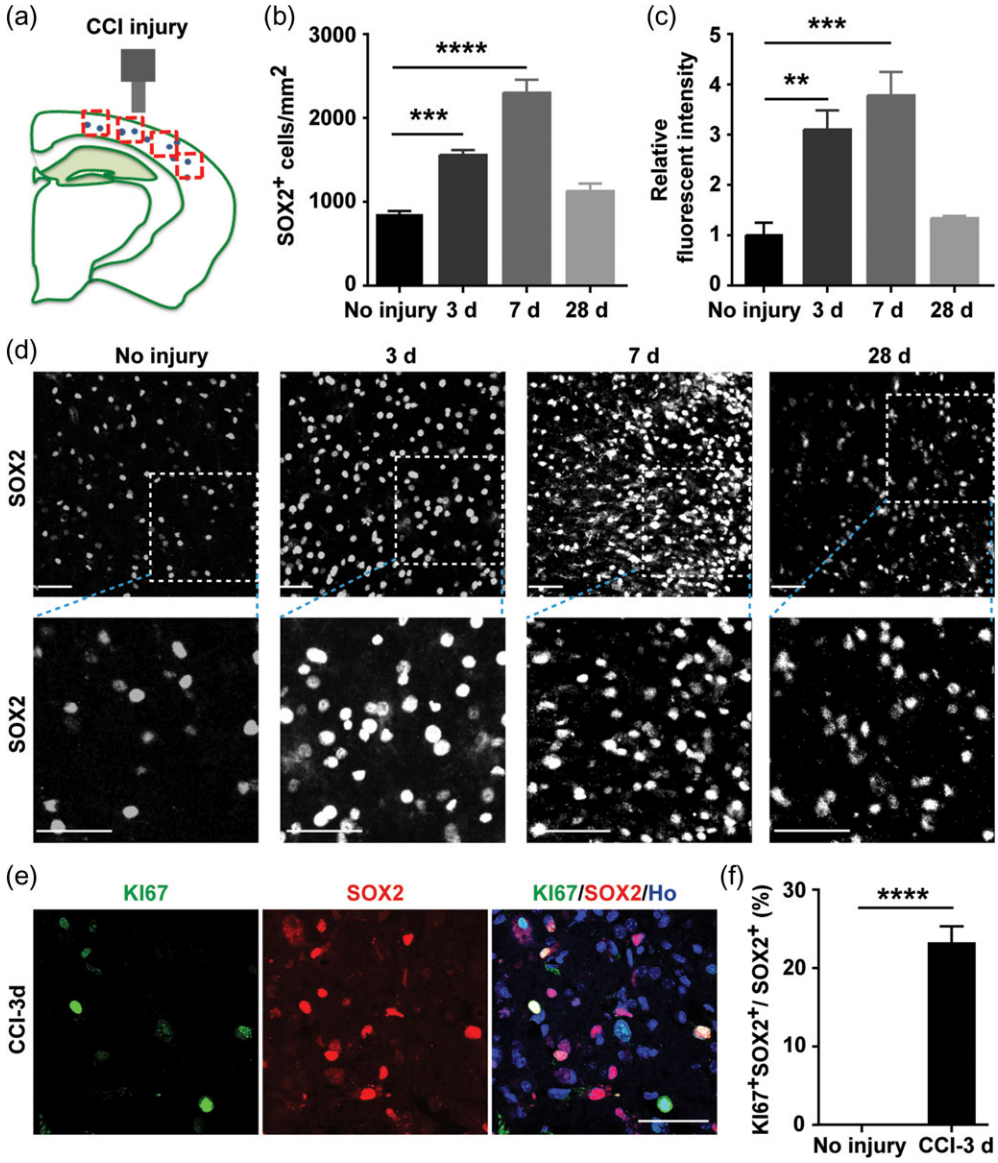

Figure 4. TBI-induced upregulation of SOX2 expression. (*a*) A schematic diagram showing controlled cortical impact (CCI)-induced TBI and counting area (red colored box) for quantification. (*b*) Density of SOX2$^+$ cells surrounding the injured cortex (means ± S.E.M., n = 3-5 mice; $F = 42.82$ and $P < 0.0001$ by one-way ANOVA; ***$P = 0.0004$ and ****$P = 0.0001$ by post hoc Tukey's test). (*c*) Enhanced SOX2 expression in cells surrounding the injured cortex (means ± S.E.M., n = 3 mice; $F = 14.71$ and $P = 0.0004$ by one-way ANOVA; **$P = 0.0032$ and ***$P = 0.0004$ by post hoc Tukey's test). (*d*) Representative confocal images of SOX2-staining in the injured cortex. Enlarged views of the boxed regions are also shown. d, days post CCI injury. (*e*, *f*) Representative images and quantification data of proliferating SOX2$^+$ cells surrounding the injury core at 3 days postinjury (dpi) (means ± S.E.M., n = 3 mice, ****$P < 0.0001$ by t-test). Scale bars: 50 μm.

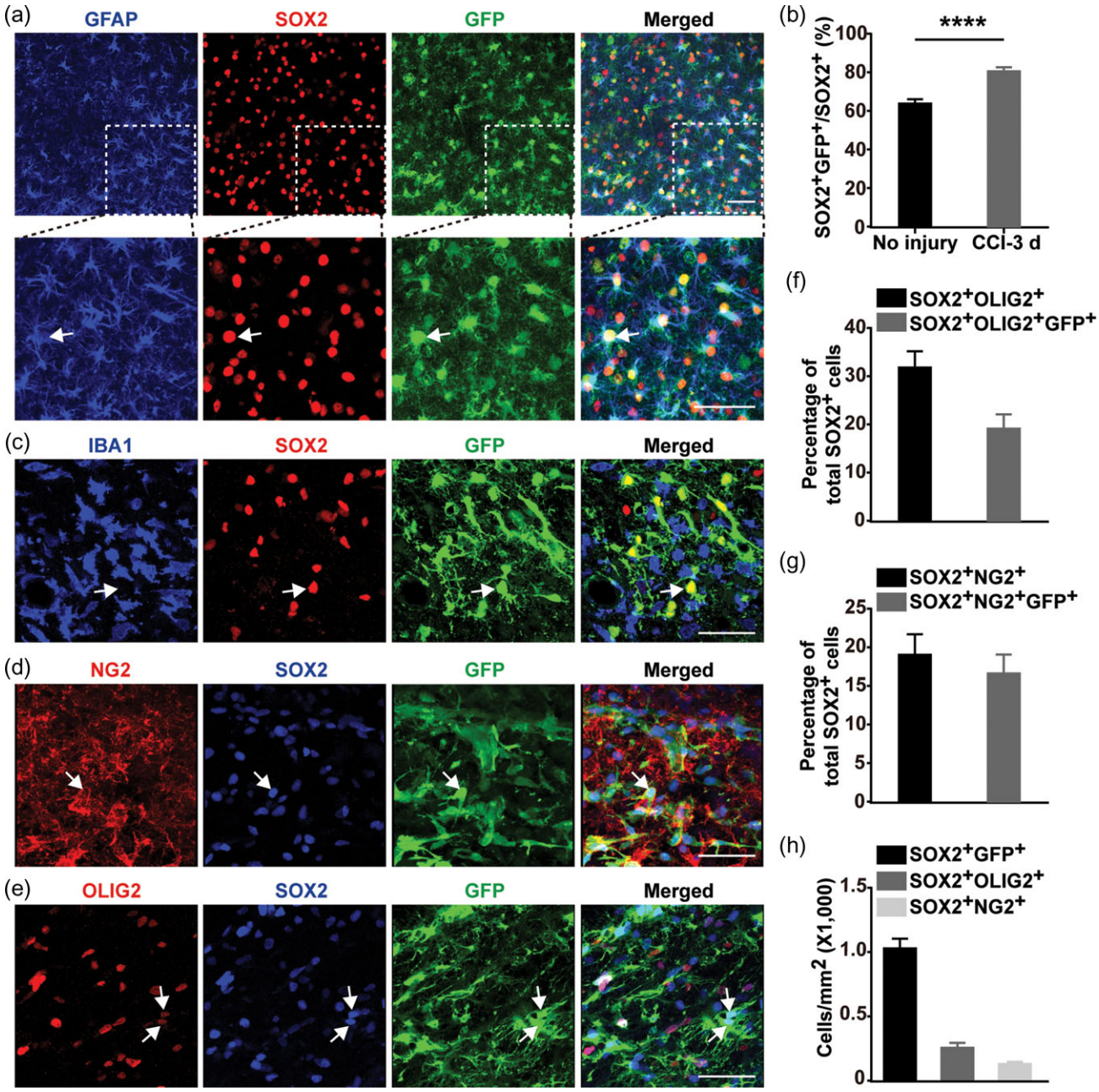

Figure 5. Broader SOX2 expression in reactive cortical glial cells. (*a*) Robust SOX2 expression in reactive cortical astrocytes, which are marked by GFAP and GFP expression in *mGfap-Cre;Rosa-YFP* mice at 3 dpi. (*b*) A predominant and increased SOX2 expression in reactive astrocytes (means ± S.E.M., $n = 3$ mice, ****$P < 0.0001$ by *t*-test). (*c*) Lack of SOX2 in reactive IBA1$^+$ microglia/macrophages. Immunohistochemistry was performed on cortical regions of *mGfap-Cre;Rosa-YFP* mice at 3 dpi. (*d*) SOX2 expression in reactive NG2$^+$ glia. Astrocytes were traced by GFP in *mGfap-Cre;Rosa-YFP* mice at 3 dpi. (*e*) SOX2 expression in OLIG2$^+$ cells. OLIG2$^+$ expression is generally weaker in SOX2$^+$ reactive astrocytes. (*f*, *g*) Relative cellular distribution of SOX2$^+$ cells in the adult cortex after TBI (means ± S.E.M., $n = 3$ mice). (*h*) Cell density of SOX2-expressing reactive glial cells (means ± S.E.M., $n = 3$ mice). Scale bars: 50 μm.

more than 1000 cells/mm^2 (Fig. 5*h*). The density for SOX2$^+$OLIG2$^+$ or SOX2$^+$NG2$^+$ cells was much lower at 256 and 129 cells/mm^2, respectively (Fig. 5*h*). Together, these results suggest that CCI induces a very robust response by SOX2$^+$ cells, with a majority of the responsive cells being reactive astrocytes.

Requirement of SOX2 for Injury-Induced Reactive Astrocytes

Proliferation is a key feature of astrogliosis following TBI (Kernie et al. 2001; Susarla et al. 2014). We firstly determined a critical time period during which a majority of reactive astrocytes undergo proliferation. We focused our analysis on the cerebral cortex because injury in this brain region causes robust SOX2 expression, although CCI might impact on both the grey and white matter (Hall et al. 2005). BrdU was administrated in drinking water from 0 to 7 days, 8 to 14 days, and 15 to 21 days after CCI (Fig. 6*a*). Reactive astrocytes were identified by staining for GFAP around the injury site. Quantification showed that astrocyte proliferation mainly occurred during the first 7 days postinjury (Fig. 6*b*). Only a very few proliferating astrocytes were detected during the following 2-time periods (Fig. 6*b*, *c*).

Therefore, we focused our further analysis on the first 7 days postinjury. Both adult *Sox2*-cKO mice and their littermate controls underwent CCI and were then administered BrdU-containing drinking water for 7 days. *Sox2*-deletion reduced proliferating reactive astrocytes by more than 50% over the first 7 days postinjury, indicated by double-staining of BrdU and GFAP around the injury core (Fig. 6*d*, *e*). The overall GFAP$^+$ reactive astrocytes were accordingly reduced by roughly 50% in *Sox2*-cKO mice, compared with wild-type controls (Fig. 6*f*). Interestingly, the average cell-body area of *Sox2*-deleted astrocytes was also significantly smaller than controls (Fig. 6*g*), indicating a reduced hypertrophic response to CCI. We then isolated astrocytes from the injured cortex 3 days after CCI and confirmed many of those SOX2-regulated candidate genes that were identified by ChIP-seq (Fig. 6*h*). These results clearly indicate that SOX2 plays a key role in activating cortical astrocytes after brain injury.

Cortical injury-induced microglia activation/macrophage recruitment was unexpectedly much reduced in *Sox2*-cKO mice (Supplementary Fig. S6a-b). The total number of microglia/macrophages surrounding the injury site decreased more than 50%, whereas those cells in proliferation reduced 65% upon inducible deletion of *Sox2*. Since *Sox2* is not expressed in microglia/macrophages, these data indicate that *Sox2*-dependent reactive astrogliosis noncell autonomously modulates microglia/macrophages after CCI. Interestingly, neuronal cell density surrounding the injury area was significantly higher in *Sox2* mutants than in wild-type controls (Supplementary Fig. S7a), although they showed no difference in NG2 glia density, cell apoptosis, or postinjury angiogenesis at 7dpi (Supplementary Figs S6c, d and S7b, c).

Sox2-Deletion in Astrocytes Promotes Functional Recovery After Injury

To determine whether SOX2 in reactive astrocytes played a role during tissue remodeling after brain injury, we analyzed glial-scar formation and lesion size surrounding the injured cortical region. Both wild-type and *Sox2*-cKO mice underwent CCI and were sacrificed for analysis 2 months later. Glial scars and lesion area were demarcated by GFAP and nuclear Hoechst3342 staining, respectively. We found that the total lesion size in the *Sox2*-cKO brains was much smaller than in the respective wild-type controls (Fig. 7*a*, *b*). Glial scars were observed in the surrounding lesion area in both wild-type and *Sox2*-cKO mice; however, the total cortical area with reactive astrocytes (GFAP$^+$ area) was significantly reduced in *Sox2*-cKO mice (Fig. 7*c*).

In addition to molecular and cellular changes, TBI also leads to behavioral deficits (Luukkainen et al. 2012; Yang et al. 2012). Accordingly, we conducted a series of neurological analysis of mice after CCI (Supplementary Fig. S8a). Overall neurological function was monitored by mNSS over time. When examined at 24 h postinjury, both *Sox2*-cKO and control mice were impaired to a nearly identical degree (Fig. 7*d*), indicating relatively uniform injuries among these mice. Interestingly, the neurological function of *Sox2*-cKO mice significantly improved during the following weeks, while their wild-type controls showed only mild gains during the first 7 days postinjury (Fig. 7*d*). When examined at 5 weeks postinjury, *Sox2*-cKO mice also spent significantly less time in immobility during the tail-suspension test, revealing much-reduced depression-like behavior (Fig. 7*e*). *Sox2*-deletion similarly improved animal performance in the elevated plus maze tests when examined at 6 weeks postinjury. *Sox2*-cKO mice stayed significantly less time in the open arm, whereas their total entries to this arm remained similar to their controls (Fig. 7*f*). Such results suggest that deletion of *Sox2* in astrocytes protects mice from CCI-induced risk-taking irrational behavior. Nonetheless, *Sox2*-cKO mice performed similarly as their wild-type controls on the hippocampus-dependent learning and memory by Morris water maze tests (Supplementary Fig. S8b, c).

Discussion

A better understanding of the molecular mechanisms controlling reactive astrocyte function is fundamental to therapeutic interventions for brain trauma. In this study, we show that the transcription factor SOX2 plays a critical role in TBI-induced reactive astrocytes. SOX2 is basally expressed in normal cortical astrocytes and highly induced by TBI. As a transcription factor, SOX2 binds to regulatory regions of many genes involved in regulating reactive astrocyte functions, such as cell cycle reentry and cytokine signaling. Injury-induced proliferation of cortical astrocytes critically requires SOX2. Since reactive gliosis is generally believed to help maintain tissue integrity after traumatic injury (Faulkner et al. 2004; Rolls et al. 2009; Burda et al. 2016), it is unexpected that conditional deletion of *Sox2* in adult astrocytes significantly reduces injury area and lesion size, and improves behavioral recovery after TBI. Therefore, our results uncover for the first time that SOX2-dependent signaling pathways in reactive astrocytes may be specifically targeted for brain recovery after traumatic injury.

SOX2 is well known for its critical role in embryonic stem cells, neural stem cells, brain development, and adult neurogenesis (Graham et al. 2003; Ferri et al. 2004; Episkopou 2005; Bani-Yaghoub et al. 2006; Pevny and Nicolis 2010). Nonetheless, its function in differentiated cells is less clear. Our analysis reveals that SOX2 is basally expressed and can be further induced by TBI in adult cortical astrocytes. This result is consistent with prior reports showing an astrocyte-enriched expression of SOX2 in both the brain and spinal cord (Bani-Yaghoub et al. 2006; Guo et al. 2011). Similar to TBI, contusion spinal cord injury and focal demyelination can also upregulate SOX2 expression in oligodendrocyte progenitor cells (OPCs) and ependymal cells (Lee et al. 2013; Zhao et al. 2015). Such induced SOX2 expression in OPCs may be required for differentiation and remyelination (Zhao et al. 2015). In addition to the central nervous system, SOX2 is detectable in GFAP$^+$ glial cells after nerve injury of the inner ear (Lang et al. 2011). Further, these injury-responsive SOX2$^+$ glial cells gain neural stem cell-like properties in culture (Lang et al. 2015). Although the exact molecular mechanism remains to be investigated, the injury-induced expression of growth factors and cytokines may be responsible for SOX2 upregulation in multiple glial cells after injury (Bani-Yaghoub et al. 2006; Srinivasan et al. 2016).

The injury-induced upregulation of SOX2 suggests it may play a unique role in astrocyte activation after brain injury. In this regard, we have recently demonstrated that SOX2 overexpression is sufficient to reprogram astrocytes into neuroblasts and functional neurons in the adult brain and spinal cord (Niu et al. 2013, 2015; Su et al. 2014; Wang et al. 2016). Brain NG2 glia can be similarly reprogrammed by ectopic SOX2 after injury (Heinrich et al. 2014). However, such neurogenic reprogramming of reactive astrocytes or NG2 glia has not been observed in spite of robust expression of endogenous SOX2 surrounding injured regions of brain or spinal cord, which suggests that an expression threshold or another yet-to-be-identified mechanism is required for this fate reprogramming in vivo. Nonetheless, SOX2 upregulation may lead to dedifferentiation of reactive astrocytes.

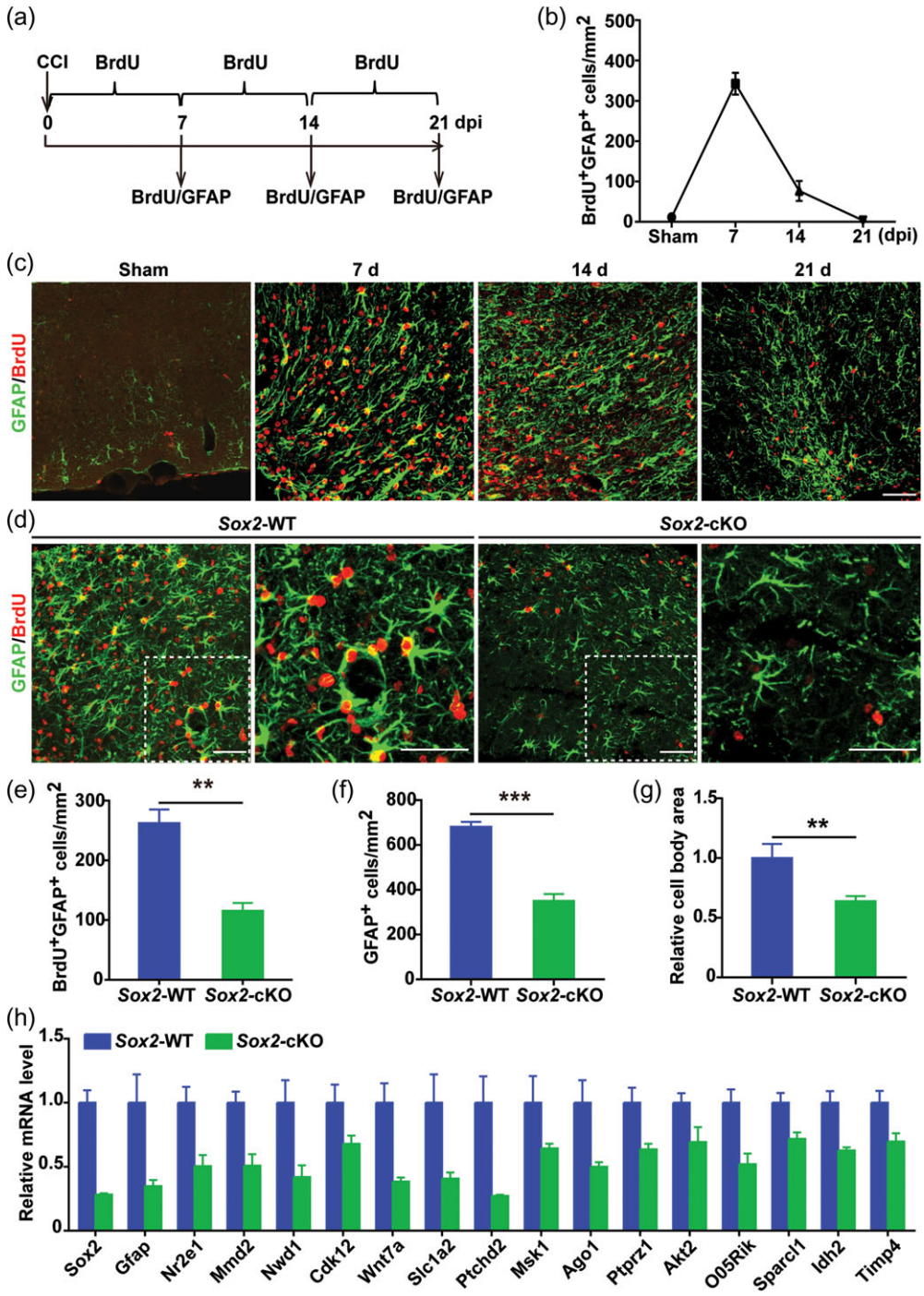

Figure 6. Astrocyte activation requires SOX2. (*a*) A strategy for analysis of astrocyte activation post CCI-induced injury. Immunohistochemistry was performed at the indicated time points. dpi, days postinjury. (*b*) Quantification of reactive astrocytes during a time course. Cells were counted surrounding the injured cortex (means ± S.E.M., $n = 4$ mice). (*c*) Representative images of activated cortical astrocytes indicated by BrdU-incorporation and GFAP staining. (*d*) Confocal images showing reduced proliferation of cortical astrocytes in mice with *Sox2*-deletion. Enlarged views of the boxed regions are shown on the respective right panels. (*e*) Quantification of proliferating cortical astrocytes at 7 dpi (means ± S.E.M., $n = 4$ mice for each genotype, $^{**}P = 0.0049$ by *t*-test). (*f*) Quantification of total activated cortical astrocytes indicated by GFAP staining at 7 dpi (means ± S.E.M., $n = 4$ mice for each genotype, $^{**}P = 0.0009$ by *t*-test). (*g*) Quantification of cell body areas of $GFAP^+$ cells at 7 dpi (means ± S.E.M., $n = 4$ mice, $^{**}P < 0.01$ by *t*-test). (*h*) Expression of SOX2 targeted genes from isolated adult cortical astrocytes 3 days after CCI (means ± S.E.M.; $n = 4$ mice; $P < 0.05$ for each of the genes by *t*-test). Scale bars: 50 μm.

Through inducible deletion of *Sox2* in adult astrocytes, we reveal for the first time an essential role of SOX2 in regulating the functions of reactive astrocytes after TBI. At the molecular level, our ChIP-seq analysis identified more than 2100 high-fidelity SOX2 bound sites in mouse cortical tissue. Since cortical astrocytes are the predominant cell type expressing SOX2 in this region, our identified binding sites largely represent SOX2 regulatory regions in these adult differentiated cells. A global GO analysis of annotated genes indicates that numerous SOX2 targets directly contribute to the regulation of the WNT, Delta-

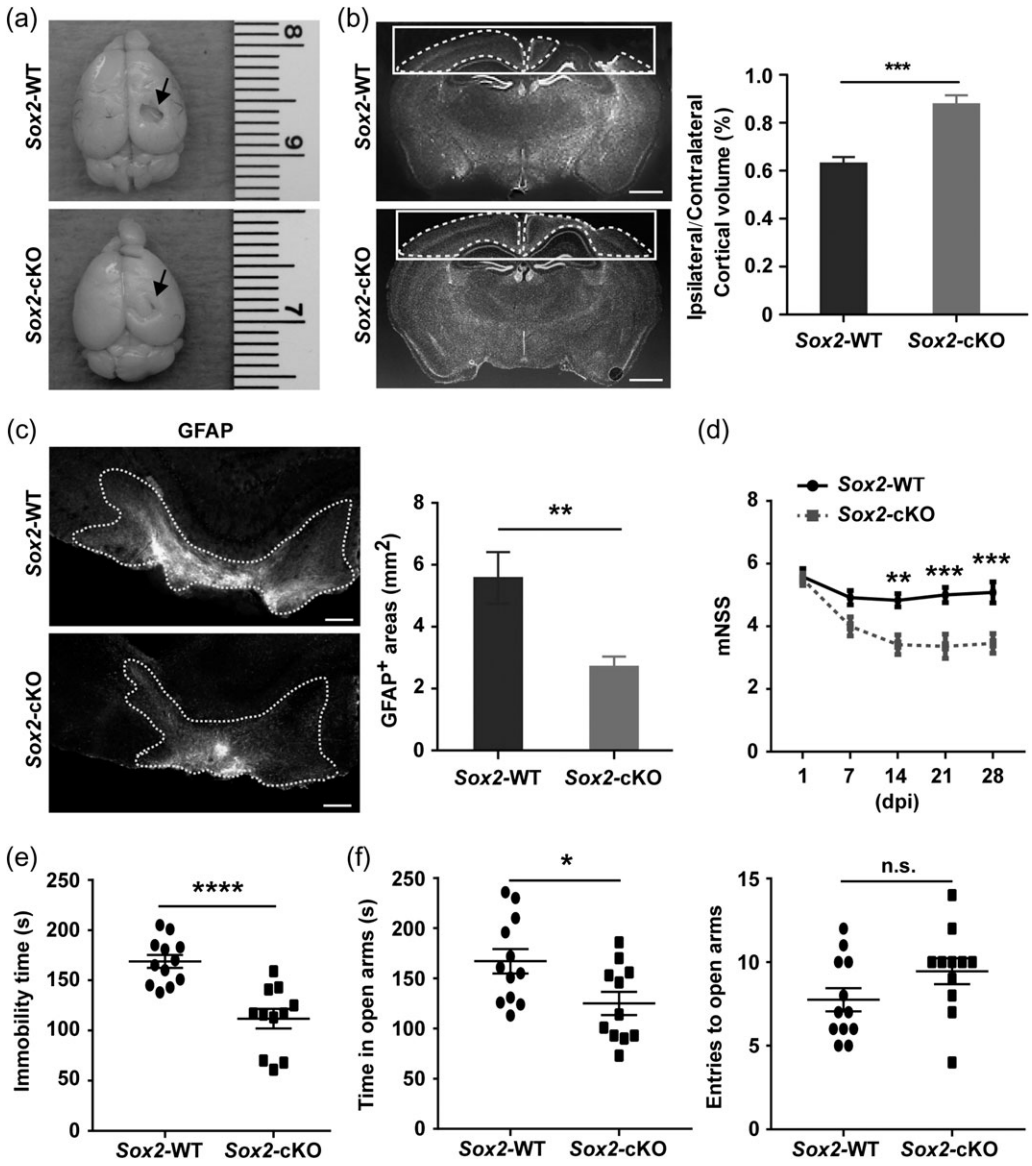

Figure 7. *Sox2*-deletion ameliorates TBI-induced functional impairments. (*a*) Whole brain overviews of the indicated mice at 2 months after CCI. The lesioned brain areas are indicated by arrows. (*b*) Quantification of lesion size. Coronal brain sections showing areas for quantification (means ± S.E.M.; $n = 5$ mice for each genotype; $^{***}P < 0.001$ by *t*-test). Scale bars: 1 mm. (*c*) Quantification of cortical areas with reactive astrogliosis. Coronal brain sections with GFAP staining showing areas for quantification. The regions with reactive gliosis are outlined by the dashed lines (means ± S.E.M.; $n = 6$ mice for each genotype; $^{**}P = 0.0098$ by *t*-test). Scale bars: 100 μm. (*d*) mNSS showing TBI-induced overall neurological impairments (means ± S.E.M.; $n = 12$ and 11 for WT and cKO mice, respectively). Data were analyzed by two-way ANOVA and post hoc Tukey's test (genotype effect: $F = 40.44$, $P < 0.0001$; time effect: $F = 8.758$, $P < 0.0001$; effect of genotype × time, $F = 2.721$, $P = 0.033$; $^{**}P < 0.01$ and $^{***}P < 0.001$). (*e*) Tail suspension test to examine depression-like behavior (means ± S.E.M.; $n = 12$ and 11 for WT and cKO mice, respectively; $^{****}P < 0.0001$ by *t*-test). (*f*) Elevated plus maze test to examine risk-taking irrational behavior (means ± S.E.M.; $n = 12$ and 11 for WT and cKO mice, respectively; $^{*}P = 0.02$ by *t*-test; n.s., not significant).

Notch, TGF-β, IL-6, and MAPK signaling pathways. These pathways are known to have critical roles in astrogenesis during normal neural development and in astrogliosis under pathological conditions (Schachtrup et al. 2010; Benner et al. 2013; Choi et al. 2013; Wanner et al. 2013; LeComte et al. 2015; Yang et al. 2016). For example, MMD2 directly regulates ERK phosphorylation and plays a key role in astrogliosis (Jin et al. 2012; Kang et al. 2012). WNT7a, a principle upstream factor activating beta-catenin, is highly expressed in astrocytes and critical for cell proliferation (Chen , Guan, Liu et al. 2012; Chen , Guan, Zhang et al. 2012). AKT2 and AKT3 are key components of PI3K/AKT and MAPK pathway, which regulates the expression of EGFR and interact with PTEN signaling, and play essential roles in regulating astrogliosis (Endersby et al. 2011; Choi et al. 2013; Xie et al. 2016). NR2E1 (also known as TLX) is enriched in adult neural stem cells and astrocytes in the adult brain with important roles in astrogliosis through regulation of the BMP signaling (Shi et al. 2004; Niu et al. 2011; Qin et al. 2014). Interestingly, the direct regulation of NR2E1 by SOX2 was previously confirmed by enhancer analysis both in cell culture and in transgenic mice (Shimozaki et al. 2012; Islam et al. 2015). Together, these results indicate that SOX2 regulates astrocyte activation by controlling the activity of multiple signaling pathways.

It is unexpected that astrocyte-specific deletion of *Sox2* in mice results in a much-reduced lesion size and significantly improved behavioral recovery after TBI. Emerging evidence

shows that reactive astrocytes are critical for restricting inflammation and preserving tissue and function (Faulkner et al. 2004; Rolls et al. 2009; Burda et al. 2016). For example, preventing astrocyte scar formation impedes recovery after spinal cord injury (Anderson et al. 2016). Ablation of proliferating reactive astrocytes leads to increased neuronal degeneration, inflammation, and tissue loss in mouse TBI models that are induced by either CCI or stab wound (Bush et al. 1999; Myer et al. 2006). Nonetheless, some studies also reveal that reactive astrogliosis contributes to secondary tissue loss, impaired regeneration, and functional disabilities (McGraw et al. 2001; Raghupathi 2004). Glial scars formed by reactive astrocytes constitute a major inhibitory environment for axonal and cellular regeneration postinjury (Bush et al. 1999; Silver and Miller 2004). For example, reducing astrogliosis and astroglial scar formation through either cell-cycle inhibition or expression of an anti-glial-scar factor increases nerve fiber growth in the core area of the injury site, and improves axonal regeneration and functional recovery after TBI or SCI (Di Giovanni et al. 2005; Jeong et al. 2012). These reported different roles of reactive astrocytes may depend on the type of injuries and very likely on the methods to manipulate the fate of reactive astrocytes. The outcome for cell-ablation-based methods may be understandably different from outcomes based on gene expression and cell-cycle regulation.

TBI results in damages to the lesion core, and molecular and cellular dysfunctions in the penumbra, which ultimately lead to behavior impairments. The mNSS measures performances of several behaviors and is generally used to evaluate neurological deficits after stroke or TBI (Chen et al. 2005; Schwarzbold et al. 2010; Ge et al. 2014). A time-course analysis of mNSS showed that *Sox2*-cKO mice recovered significantly better than controls. Emotional behaviors associated with the prefrontal cortex, which are frequently impaired in animals with TBI-induced cortical injuries (Schwarzbold et al. 2010; Washington et al. 2012; Huang et al. 2013), can be assessed through elevated plus maze and tail suspension tests (Schwarzbold et al. 2010; Adhikari et al. 2011). In both of these paradigms, *Sox2*-cKO mice were less impaired. In contrast, *Sox2*-deletion has no significant effect on hippocampus-dependent learning and memory measured by MWM tests. Together, these data indicate that SOX2-mediated response in astrocytes exacerbates certain functional deficits after cortical injury.

In summary, our results reveal that SOX2 plays an important role in TBI-induced reactive gliosis and behavioral deficits. They further suggest that the SOX2-dependent pathways may be specifically targeted for recovery after TBI.

Supplementary Material

Supplementary data is available at *Cerebral Cortex* online.

Authors' Contributions

C.C., S.Q., and C.-L.Z. conceived and designed the experiments. C.C., X.Z., D.K.S., W.T., J.Y., J.S., and S.Q. performed the experiments and analyzed the data. L.-L.W. provided critical reagents and scientific inputs. Y.Z. maintained mouse colonies. C.C., X.Z., S.Q., and C.-L.Z prepared the article. All authors reviewed and approved the article.

Funding

The work in the Zhang laboratory was supported by Welch Foundation (I-1724), Texas Institute for Brain Injury and Repair, Decherd Foundation, Kent Waldrep Foundation Center for Basic Research on Nerve Growth and Regeneration, Mobility Foundation, National Institutes of Health (NS070981, NS099073, NS088095, NS092616, and NS093502) and National Natural Science Foundation of China (No.81528006). The work in the Qin laboratory was supported by grants from National Key Basic Research Program of China (973 Program, No.2014CB965001), National Natural Science Foundation of China (No.81528006), and Fundamental Research Funds for the Central Universities (No. 1501219100).

Notes

We thank members of the Zhang laboratory for discussions and reagents and Dr Shari Birnbaum at the Rodent Behavior Core Facility at UT Southwestern for behavior analysis. C-.L.Z. is a W. W. Caruth, Jr Scholar in Biomedical Research. *Conflict of Interest*: None declared.

References

Adhikari A, Topiwala MA, Gordon JA. 2011. Single units in the medial prefrontal cortex with anxiety-related firing patterns are preferentially influenced by ventral hippocampal activity. Neuron. 71:898–910.

Anderson MA, Burda JE, Ren Y, Ao Y, O'Shea TM, Kawaguchi R, Coppola G, Khakh BS, Deming TJ, Sofroniew MV. 2016. Astrocyte scar formation aids central nervous system axon regeneration. Nature. 532:195–200.

Avilion AA, Nicolis SK, Pevny LH, Perez L, Vivian N, Lovell-Badge R. 2003. Multipotent cell lineages in early mouse development depend on SOX2 function. Genes Dev. 17: 126–140.

Bani-Yaghoub M, Tremblay RG, Lei JX, Zhang D, Zurakowski B, Sandhu JK, Smith B, Ribecco-Lutkiewicz M, Kennedy J, Walker PR, et al. 2006. Role of Sox2 in the development of the mouse neocortex. Dev Biol. 295:52–66.

Benner EJ, Luciano D, Jo R, Abdi K, Paez-Gonzalez P, Sheng H, Warner DS, Liu C, Eroglu C, Kuo CT. 2013. Protective astrogenesis from the SVZ niche after injury is controlled by Notch modulator Thbs4. Nature. 497:369–373.

Buffo A, Rolando C, Ceruti S. 2010. Astrocytes in the damaged brain: molecular and cellular insights into their reactive response and healing potential. Biochem Pharmacol. 79: 77–89.

Burda JE, Bernstein AM, Sofroniew MV. 2016. Astrocyte roles in traumatic brain injury. Exp Neurol. 275(Pt 3):305–315.

Burda JE, Sofroniew MV. 2014. Reactive gliosis and the multicellular response to CNS damage and disease. Neuron. 81: 229–248.

Bush TG, Puvanachandra N, Horner CH, Polito A, Ostenfeld T, Svendsen CN, Mucke L, Johnson MH, Sofroniew MV. 1999. Leukocyte infiltration, neuronal degeneration, and neurite outgrowth after ablation of scar-forming, reactive astrocytes in adult transgenic mice. Neuron. 23:297–308.

Bylund M, Andersson E, Novitch BG, Muhr J. 2003. Vertebrate neurogenesis is counteracted by Sox1-3 activity. Nat Neurosci. 6:1162–1168.

Can A, Dao DT, Terrillion CE, Piantadosi SC, Bhat S, Gould TD. 2012. The tail suspension test. J Vis Exp. 59:e3769.

Chen J, Zhang C, Jiang H, Li Y, Zhang L, Robin A, Katakowski M, Lu M, Chopp M. 2005. Atorvastatin induction of VEGF and BDNF promotes brain plasticity after stroke in mice. J Cereb Blood Flow Metab. 25:281–290.

Chen Y, Guan Y, Liu H, Wu X, Yu L, Wang S, Zhao C, Du H, Wang X. 2012. Activation of the Wnt/beta-catenin signaling pathway is associated with glial proliferation in the adult spinal cord of ALS transgenic mice. Biochem Biophys Res Commun. 420:397–403.

Chen Y, Guan Y, Zhang Z, Liu H, Wang S, Yu L, Wu X, Wang X. 2012. Wnt signaling pathway is involved in the pathogenesis of amyotrophic lateral sclerosis in adult transgenic mice. Neurol Res. 34:390–399.

Choi I, Kim J, Jeong HK, Kim B, Jou I, Park SM, Chen L, Kang UJ, Zhuang X, Joe EH. 2013. PINK1 deficiency attenuates astrocyte proliferation through mitochondrial dysfunction, reduced AKT and increased p38 MAPK activation, and downregulation of EGFR. Glia. 61:800–812.

Clausen F, Hanell A, Israelsson C, Hedin J, Ebendal T, Mir AK, Gram H, Marklund N. 2011. Neutralization of interleukin-1beta reduces cerebral edema and tissue loss and improves late cognitive outcome following traumatic brain injury in mice. Eur J Neurosci. 34:110–123.

Di Giovanni S, Movsesyan V, Ahmed F, Cernak I, Schinelli S, Stoica B, Faden AI. 2005. Cell cycle inhibition provides neuroprotection and reduces glial proliferation and scar formation after traumatic brain injury. Proc Natl Acad Sci USA. 102:8333–8338.

Endersby R, Zhu X, Hay N, Ellison DW, Baker SJ. 2011. Nonredundant functions for Akt isoforms in astrocyte growth and gliomagenesis in an orthotopic transplantation model. Cancer Res. 71:4106–4116.

Episkopou V. 2005. SOX2 functions in adult neural stem cells. Trends Neurosci. 28:219–221.

Faulkner JR, Herrmann JE, Woo MJ, Tansey KE, Doan NB, Sofroniew MV. 2004. Reactive astrocytes protect tissue and preserve function after spinal cord injury. J Neurosci. 24: 2143–2155.

Ferri AL, Cavallaro M, Braida D, Di Cristofano A, Canta A, Vezzani A, Ottolenghi S, Pandolfi PP, Sala M, DeBiasi S, et al. 2004. Sox2 deficiency causes neurodegeneration and impaired neurogenesis in the adult mouse brain. Development. 131:3805–3819.

Ganat YM, Silbereis J, Cave C, Ngu H, Anderson GM, Ohkubo Y, Ment LR, Vaccarino FM. 2006. Early postnatal astroglial cells produce multilineage precursors and neural stem cells in vivo. J Neurosci. 26:8609–8621.

Ge XT, Lei P, Wang HC, Zhang AL, Han ZL, Chen X, Li SH, Jiang RC, Kang CS, Zhang JN. 2014. miR-21 improves the neurological outcome after traumatic brain injury in rats. Sci Rep. 4: 6718.

Gong S, Zheng C, Doughty ML, Losos K, Didkovsky N, Schambra UB, Nowak NJ, Joyner A, Leblanc G, Hatten ME, et al. 2003. A gene expression atlas of the central nervous system based on bacterial artificial chromosomes. Nature. 425:917–925.

Graham V, Khudyakov J, Ellis P, Pevny L. 2003. SOX2 functions to maintain neural progenitor identity. Neuron. 39: 749–765.

Gregorian C, Nakashima J, Le Belle J, Ohab J, Kim R, Liu A, Smith KB, Groszer M, Garcia AD, Sofroniew MV, et al. 2009. Pten deletion in adult neural stem/progenitor cells enhances constitutive neurogenesis. J Neurosci. 29:1874–1886.

Gubbay J, Collignon J, Koopman P, Capel B, Economou A, Munsterberg A, Vivian N, Goodfellow P, Lovell-Badge R. 1990. A gene mapping to the sex-determining region of the mouse Y chromosome is a member of a novel family of embryonically expressed genes. Nature. 346:245–250.

Guo F, Maeda Y, Ma J, Delgado M, Sohn J, Miers L, Ko EM, Bannerman P, Xu J, Wang Y, et al. 2011. Macroglial plasticity and the origins of reactive astroglia in experimental autoimmune encephalomyelitis. J Neurosci. 31:11914–11928.

Hall ED, Sullivan PG, Gibson TR, Pavel KM, Thompson BM, Scheff SW. 2005. Spatial and temporal characteristics of neurodegeneration after controlled cortical impact in mice: more than a focal brain injury. J Neurotrauma. 22:252–265.

Heinrich C, Bergami M, Gascon S, Lepier A, Vigano F, Dimou L, Sutor B, Berninger B, Gotz M. 2014. Sox2-mediated conversion of NG2 glia into induced neurons in the injured adult cerebral cortex. Stem Cell Rep. 3:1000–1014.

Huang XT, Zhang YQ, Li SJ, Li SH, Tang Q, Wang ZT, Dong JF, Zhang JN. 2013. Intracerebroventricular transplantation of ex vivo expanded endothelial colony-forming cells restores blood-brain barrier integrity and promotes angiogenesis of mice with traumatic brain injury. J Neurotrauma. 30: 2080–2088.

Islam MM, Smith DK, Niu W, Fang S, Iqbal N, Sun G, Shi Y, Zhang CL. 2015. Enhancer analysis unveils genetic interactions between TLX and SOX2 in neural stem cells and in vivo reprogramming. Stem Cell Rep. 5:805–815.

Jeong SR, Kwon MJ, Lee HG, Joe EH, Lee JH, Kim SS, Suh-Kim H, Kim BG. 2012. Hepatocyte growth factor reduces astrocytic scar formation and promotes axonal growth beyond glial scars after spinal cord injury. Exp Neurol. 233:312–322.

Jin T, Ding Q, Huang H, Xu D, Jiang Y, Zhou B, Li Z, Jiang X, He J, Liu W, et al. 2012. PAQR10 and PAQR11 mediate Ras signaling in the Golgi apparatus. Cell Res. 22:661–676.

Kang P, Lee HK, Glasgow SM, Finley M, Donti T, Gaber ZB, Graham BH, Foster AE, Novitch BG, Gronostajski RM, et al. 2012. Sox9 and NFIA coordinate a transcriptional regulatory cascade during the initiation of gliogenesis. Neuron. 74: 79–94.

Kang W, Balordi F, Su N, Chen L, Fishell G, Hebert JM. 2014. Astrocyte activation is suppressed in both normal and injured brain by FGF signaling. Proc Natl Acad Sci USA. 111: E2987–E2995.

Kernie SG, Erwin TM, Parada LF. 2001. Brain remodeling due to neuronal and astrocytic proliferation after controlled cortical injury in mice. J Neurosci Res. 66:317–326.

Kondo A, Shahpasand K, Mannix R, Qiu J, Moncaster J, Chen CH, Yao Y, Lin YM, Driver JA, Sun Y, et al. 2015. Antibody against early driver of neurodegeneration cis P-tau blocks brain injury and tauopathy. Nature. 523:431–436.

Lang H, Li M, Kilpatrick LA, Zhu J, Samuvel DJ, Krug EL, Goddard JC. 2011. Sox2 up-regulation and glial cell proliferation following degeneration of spiral ganglion neurons in the adult mouse inner ear. J Assoc Res Otolaryngol. 12:151–171.

Lang H, Xing Y, Brown LN, Samuvel DJ, Panganiban CH, Havens LT, Balasubramanian S, Wegner M, Krug EL, Barth JL. 2015. Neural stem/progenitor cell properties of glial cells in the adult mouse auditory nerve. Sci Rep. 5:13383.

LeComte MD, Shimada IS, Sherwin C, Spees JL. 2015. Notch1-STAT3-ETBR signaling axis controls reactive astrocyte proliferation after brain injury. Proc Natl Acad Sci USA. 112: 8726–8731.

Lee HJ, Wu J, Chung J, Wrathall JR. 2013. SOX2 expression is upregulated in adult spinal cord after contusion injury in both oligodendrocyte lineage and ependymal cells. J Neurosci Res. 91:196–210.

Luukkainen S, Riala K, Laukkanen M, Hakko H, Rasanen P. 2012. Association of traumatic brain injury with criminality in

adolescent psychiatric inpatients from Northern Finland. Psychiatry Res. 200:767–772.

Madisen L, Zwingman TA, Sunkin SM, Oh SW, Zariwala HA, Gu H, Ng LL, Palmiter RD, Hawrylycz MJ, Jones AR, et al. 2010. A robust and high-throughput Cre reporting and characterization system for the whole mouse brain. Nat Neurosci. 13:133–140.

McGraw J, Hiebert GW, Steeves JD. 2001. Modulating astrogliosis after neurotrauma. J Neurosci Res. 63:109–115.

Myer DJ, Gurkoff GG, Lee SM, Hovda DA, Sofroniew MV. 2006. Essential protective roles of reactive astrocytes in traumatic brain injury. Brain. 129:2761–2772.

Niu W, Zang T, Smith DK, Vue TY, Zou Y, Bachoo R, Johnson JE, Zhang CL. 2015. SOX2 reprograms resident astrocytes into neural progenitors in the adult brain. Stem Cell Rep. 4: 780–794.

Niu W, Zang T, Zou Y, Fang S, Smith DK, Bachoo R, Zhang CL. 2013. In vivo reprogramming of astrocytes to neuroblasts in the adult brain. Nat Cell Biol. 15:1164–1175.

Niu W, Zou Y, Shen C, Zhang CL. 2011. Activation of postnatal neural stem cells requires nuclear receptor TLX. J Neurosci. 31:13816–13828.

Pardo L, Schluter A, Valor LM, Barco A, Giralt M, Golbano A, Hidalgo J, Jia P, Zhao Z, Jove M, et al. 2016. Targeted activation of CREB in reactive astrocytes is neuroprotective in focal acute cortical injury. Glia. 64:853–874.

Pekny M, Pekna M. 2014. Astrocyte reactivity and reactive astrogliosis: costs and benefits. Physiol Rev. 94:1077–1098.

Pevny LH, Nicolis SK. 2010. Sox2 roles in neural stem cells. Int J Biochem Cell Biol. 42:421–424.

Qin S, Niu W, Iqbal N, Smith DK, Zhang CL. 2014. Orphan nuclear receptor TLX regulates astrogenesis by modulating BMP signaling. Front Neurosci. 8:74.

Raghupathi R. 2004. Cell death mechanisms following traumatic brain injury. Brain Pathol. 14:215–222.

Ridet JL, Malhotra SK, Privat A, Gage FH. 1997. Reactive astrocytes: cellular and molecular cues to biological function. Trends Neurosci. 20:570–577.

Rolls A, Shechter R, Schwartz M. 2009. The bright side of the glial scar in CNS repair. Nat Rev Neurosci. 10:235–241.

Schachtrup C, Ryu JK, Helmrick MJ, Vagena E, Galanakis DK, Degen JL, Margolis RU, Akassoglou K. 2010. Fibrinogen triggers astrocyte scar formation by promoting the availability of active TGF-beta after vascular damage. J Neurosci. 30: 5843–5854.

Schildge S, Bohrer C, Beck K, Schachtrup C. 2013. Isolation and culture of mouse cortical astrocytes. J Vis Exp. 71:e50079.

Schwarzbold ML, Rial D, De Bem T, Machado DG, Cunha MP, dos Santos AA, dos Santos DB, Figueiredo CP, Farina M, Goldfeder EM, et al. 2010. Effects of traumatic brain injury of different severities on emotional, cognitive, and oxidative stress-related parameters in mice. J Neurotrauma. 27: 1883–1893.

Shaham O, Smith AN, Robinson ML, Taketo MM, Lang RA, Ashery-Padan R. 2009. Pax6 is essential for lens fiber cell differentiation. Development. 136:2567–2578.

Shi Y, Chichung Lie D, Taupin P, Nakashima K, Ray J, Yu RT, Gage FH, Evans RM. 2004. Expression and function of orphan nuclear receptor TLX in adult neural stem cells. Nature. 427: 78–83.

Shimozaki K, Zhang CL, Suh H, Denli AM, Evans RM, Gage FH. 2012. SRY-box-containing gene 2 regulation of nuclear receptor tailless (Tlx) transcription in adult neural stem cells. J Biol Chem. 287:5969–5978.

Silver J, Miller JH. 2004. Regeneration beyond the glial scar. Nat Rev Neurosci. 5:146–156.

Sofroniew MV. 2009. Molecular dissection of reactive astrogliosis and glial scar formation. Trends Neurosci. 32:638–647.

Sofroniew MV, Vinters HV. 2010. Astrocytes: biology and pathology. Acta Neuropathol. 119:7–35.

Srinivas S, Watanabe T, Lin CS, William CM, Tanabe Y, Jessell TM, Costantini F. 2001. Cre reporter strains produced by targeted insertion of EYFP and ECFP into the ROSA26 locus. BMC Dev Biol. 1:4.

Srinivasan K, Friedman BA, Larson JL, Lauffer BE, Goldstein LD, Appling LL, Borneo J, Poon C, Ho T, Cai F, et al. 2016. Untangling the brain's neuroinflammatory and neurodegenerative transcriptional responses. Nat Commun. 7:11295.

Su Z, Niu W, Liu ML, Zou Y, Zhang CL. 2014. In vivo conversion of astrocytes to neurons in the injured adult spinal cord. Nat Commun. 5:3338.

Suh H, Consiglio A, Ray J, Sawai T, D'Amour KA, Gage FH. 2007. In vivo fate analysis reveals the multipotent and self-renewal capacities of Sox2+ neural stem cells in the adult hippocampus. Cell Stem Cell. 1:515–528.

Susarla BT, Villapol S, Yi JH, Geller HM, Symes AJ. 2014. Temporal patterns of cortical proliferation of glial cell populations after traumatic brain injury in mice. ASN Neuro. 6: 159–170.

Tanaka S, Kamachi Y, Tanouchi A, Hamada H, Jing N, Kondoh H. 2004. Interplay of SOX and POU factors in regulation of the Nestin gene in neural primordial cells. Mol Cell Biol. 24: 8834–8846.

Tsai HH, Li H, Fuentealba LC, Molofsky AV, Taveira-Marques R, Zhuang H, Tenney A, Murnen AT, Fancy SP, Merkle F, et al. 2012. Regional astrocyte allocation regulates CNS synaptogenesis and repair. Science. 337:358–362.

Tweedie D, Rachmany L, Rubovitch V, Zhang Y, Becker KG, Perez E, Hoffer BJ, Pick CG, Greig NH. 2013. Changes in mouse cognition and hippocampal gene expression observed in a mild physical- and blast-traumatic brain injury. Neurobiol Dis. 54:1–11.

Walf AA, Frye CA. 2007. The use of the elevated plus maze as an assay of anxiety-related behavior in rodents. Nat Protoc. 2:322–328.

Wang LL, Su Z, Tai W, Zou Y, Xu XM, Zhang CL. 2016. The p53 pathway controls SOX2-mediated reprogramming in the adult mouse spinal cord. Cell Rep. 17:891–903.

Wang TW, Stromberg GP, Whitney JT, Brower NW, Klymkowsky MW, Parent JM. 2006. Sox3 expression identifies neural progenitors in persistent neonatal and adult mouse forebrain germinative zones. J Comp Neurol. 497:88–100.

Wanner IB, Anderson MA, Song B, Levine J, Fernandez A, Gray-Thompson Z, Ao Y, Sofroniew MV. 2013. Glial scar borders are formed by newly proliferated, elongated astrocytes that interact to corral inflammatory and fibrotic cells via STAT3-dependent mechanisms after spinal cord injury. J Neurosci. 33:12870–12886.

Washington PM, Forcelli PA, Wilkins T, Zapple DN, Parsadanian M, Burns MP. 2012. The effect of injury severity on behavior: a phenotypic study of cognitive and emotional deficits after mild, moderate, and severe controlled cortical impact injury in mice. J Neurotrauma. 29:2283–2296.

Xie ZF, Xin G, Xu YX, Su Y, Li KS. 2016. LPS-primed release of HMGB-1 from cortical astrocytes is modulated through PI3K/AKT pathway. Cell Mol Neurobiol. 36:93–102.

Xiong Y, Mahmood A, Chopp M. 2013. Animal models of traumatic brain injury. Nat Rev Neurosci. 14:128–142.

Yang CC, Hua MS, Lin WC, Tsai YH, Huang SJ. 2012. Irritability following traumatic brain injury: divergent manifestations of annoyance and verbal aggression. Brain Inj. 26:1185–1191.

Yang J, Zhang X, Wu Y, Zhao B, Liu X, Pan Y, Liu Y, Ding Y, Qiu M, Wang YZ, et al. 2016. Wnt/beta-catenin signaling mediates the seizure-facilitating effect of postischemic reactive astrocytes after pentylenetetrazole-kindling. Glia. 64:1083–1091.

Zhang CL, Zou Y, He W, Gage FH, Evans RM. 2008. A role for adult TLX-positive neural stem cells in learning and behaviour. Nature. 451:1004–1007.

Zhao C, Ma D, Zawadzka M, Fancy SP, Elis-Williams L, Bouvier G, Stockley JH, de Castro GM, Wang B, Jacobs S, Casaccia P, et al. 2015. Sox2 sustains recruitment of oligodendrocyte progenitor cells following CNS demyelination and primes them for differentiation during remyelination. J Neurosci. 35:11482–11499.